Design of A Rollable Antenna System for Satellite

Ashwaq Alkaabi[1], Abdul-Halim Jallad[2], Mostafa El Sayed[3], Adriano Camps[4,5,6]
[1]United Arab Emirates University, CoS, POBox 15551 Al-Ain, UAE
[2]United Arab Emirates University, CoE, POBox 15551 Al-Ain, UAE
[3]Carleton University, 1125 Colonel By Drive, Ottawa, Ontario, K1S 5B6 Canada
[4]CommSensLab – UPC, Universitat Politècnica de Catalunya – BarcelonaTech, Barcelona, Spain
[5]Institut d'Estudis Espacials de Catalunya (IEEC) – CTE-UPC, E-08034 Barcelona, Spain
[6]ASPIRE Visiting International Professor, UAE University, CoE, POBox 15551 Al-Ain, UAE

***Abstract*— This paper presents the development of a deployable Synthetic Aperture Radar (SAR) antenna tailored for a 16U CubeSat platform. The primary challenge addressed the need for large antennas in SAR satellites, which traditionally increase satellite size and cost to achieve high-resolution imaging. The proposed solution is a scalable 4×21 patch antenna array operating at 1.275 GHz, integrated into a flexible polyimide-based printed circuit board (PCB). This flexible design enables compact storage by allowing the antenna to roll during deployment, overcoming the limitations of rigid PCBs. However, polyimide's higher losses and suboptimal performance than other microstrip substrates, such as FR4 and Rogers, pose challenges. Impedance matching is achieved using a quarter-wave transformer, and precise element spacing prevents field interference. Mechanically, the design leverages the bending properties of polyimide to fit the antenna within 8U of the CubeSat, with previous work ensuring that rolling does not affect the antenna's structural integrity or torque during flight. Initial simulations using CST software for a 4×2 array show promising results, with future work aiming to prototype a 4×4 array. This flexible, scalable antenna design promises to reduce satellite size and cost while maintaining or enhancing SAR performance, offering a cost-effective solution for spaceborne radar applications and Earth observation.**

Keywords—SAR, patch antenna array, flexible PCB, CST simulations, CubeSat.

I. INTRODUCTION

In modern wireless communication systems, the demand for high-performance antennas tailored to specific frequency bands is ever-growing. This paper describes the design, analysis, and evaluation of a microstrip patch antenna array meticulously optimized for operation at 1.275 GHz. Amidst the vast landscape of electromagnetic spectrum utilization, the 1.275 GHz frequency band holds particular significance, finding applications in radio-localization, radio-navigation (space-Earth and space-space), active satellite Earth Observation, and active space research. Against this backdrop, the design considerations encompass the electromagnetic properties of the antenna array and the mechanical constraints. [3].

II. DESIGN METHODOLOGY

The design of the SAR antenna array was conducted by taking into account the mechanical and RF systems. The first aspect was the mechanical side of the design, it was important to give the design certain constraints and limitations; in this case, it was the 8U CubeSat. On the other hand, the frequency selection for the SAR system did vary as the L-band and P-bands of the SAR antenna have higher penetration as compared to the higher bands, however, the P-band will lead to a larger antenna as compared to the L-band, making the L-band a better-suited size. According to the ITU and United Arab Emirates's telecommunication regulation, the range operating for SAR missions is 1.215 GHz to 1.300 which is allocated for Exploration-Satellite Service (EESS) [5]. For the following frequency range, the width was calculated to be between 5.898 and 6.796 cm, and based on NASA's Seasat mission, and many other missions, the central frequency was chosen to be 1.275 GHz [6].

A. Mechanical design constraints

The SAR system will be integrated within the 8U CubeSat, a 10 x 20 x 40 cm, leaving the other 8U for the satellite avionics. Moreover, as the design will be integrated within a commercial CubeSat supplier, most suppliers of 16U structure their CubeSat at 226.3 x 226.3 x 454 mm [7].

1) Deployed Structure

The length of the deployed structure was determined based on previous work, which specified a length of 4 meters [2]. This aligns with the typical size of SAR antennas, which varies by frequency band and the optimum azimuthal spatial resolution. At L-band SAR, with a wavelength of 15 to 30 cm, antennas generally range from 3 to 10 meters for spaceborne systems. In contrast, C-band SAR has a shorter wavelength (3.75 to 7.5 cm) and typically uses antennas between 1 and 5 meters. X-band SAR systems, with an even shorter wavelength, have antennas measuring between 1 and 3 meters [1] [8].

The length of the antenna is critical and requires many trade-offs, as the best spatial resolution found is half the antenna length. However, the size affects both the Doppler effect and the pulse repetition frequency [9]. For instance, the C-band antenna on Sentinel-1 is 12.3 meters long [10], and the RADARSAT-2 C-band antenna measures 15 meters [11]. Both satellites are large, complex systems weighing over 2,000 kg and costing hundreds of millions of dollars to develop and launch.

2) PCB Type

Flexible PCBs are used in the design, as they will be stowed, and then deployed in flight. There are three kinds of flexible PCBs, a dynamic PCB with frequent possibilities of bending, a semi-dynamic which can bend/unbend for a maximum of 20 times, and a stable PCB which is bent only once as it has a rigid part. Since the design will be rolled on itself, and unrolled, the stable PCB is not an option. It was also advised to have a specific bending radius which depends on the PCB's type, and after the initial CAD drawing, it was found that a larger bending radius (r) is required, determining that the dynamic PCB is the optimal option [12]. The dynamic PCB has a bending radius that is between 25 – 100 times the thickness of the PCB (h), and by IPC-2223B, the recommended ratio of r/h is 25. In this design, the thickness of the Flexible Printed Circuit (FPC) is 2 mm, resulting in a minimum bending radius of 50 mm. This bending radius is introduced to the design to induce a curvature in the full length of the PCB, resulting in a natural deployment of the structure, as it will roll easily without any additional forces, the curvature will also add stiffness to the antenna array sheet [2].

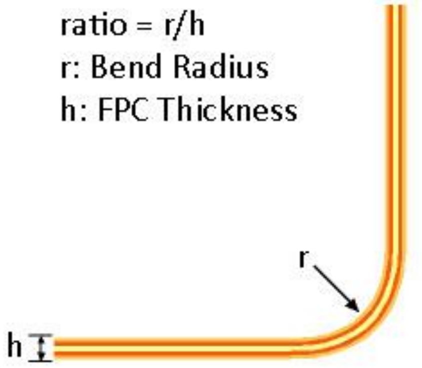

Figure 1 Bend Radius

3) Stowed/Rolled configuration

The stowed configuration is to be integrated within the 126.3 x 226.3 x 454 mm^3 space, and the method of stowing will be by rolling the deployed structure. As the PCB was decided to be a dynamic flexible PCB, it will not break due to the stress resulting from the rolling/deploying. Following the concern above, the height of the rolled configuration should not exceed 126.3 mm and have a depth of 226.3 mm as seen in Figure 2. The number of rolls seen in the Figure was found using the simple equation, and using this number the total height (H) was found. However, as the height is one of the constraints, it was traded as the known variable to find the number of desired rolls, as the number can be controlled using the angle between the rolled structure and the portion of the sheet attached to the CubeSat.

$$n = \sqrt{\left(\frac{r_i}{h}\right)^2 + \frac{L_i}{\pi h}} - \frac{r_i}{h}, \quad (1)$$

$$H = D + (h \, x \, n \, x \, 2), \quad (2)$$

n represents the number of rolls (coils), r_i is the bending radius, h is the PCB thickness, and L_i is the deployed length, the height H was manually calculated as a function of D=2r_i, and the r_i and h are illustrated in Figure 1. This resulted in a maximum number of rolls to be 10, to maintain the height required.

B. Array Configuration

Element spacing is critical in antenna arrays, as improper distances between patches can lead to grating lobes and affect performance. For optimal results, the spacing is typically 50-65% of the wavelength in a vacuum, measured from the center of one patch to another. At 1.275 GHz, this corresponds to a wavelength of 23.5 cm, resulting in a patch spacing between 11–15 cm. However, in a compact design with 4 patches per row and a very tight width, the patch spacing will not fit. Therefore, the substrate effect was considered as it changes the wavelength due to its dielectric constant, and for a polyimide substrate (ε_r = 3.5), the effective wavelength is reduced to 12.56 cm. Thus, the new patch spacing is between 6.3 and 8.1 cm.

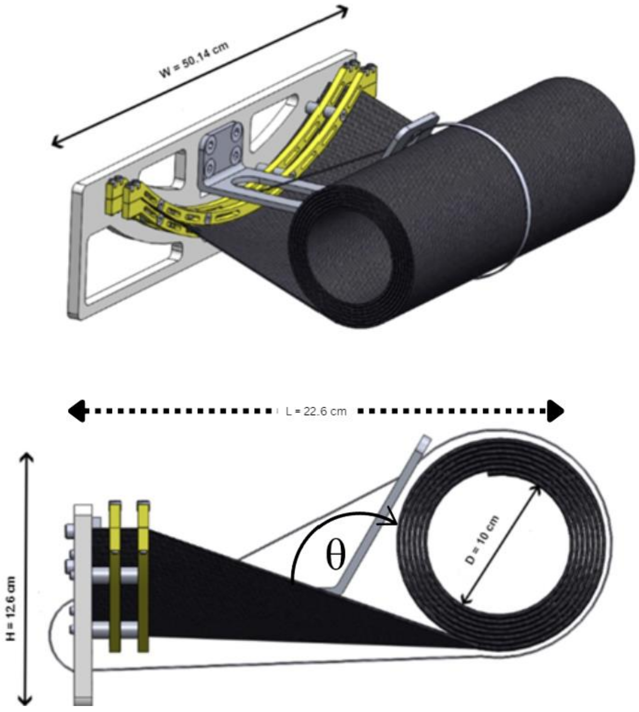

Figure 2 3D model of Stowed Configuration

The number of elements in the array influences gain but also increases design complexity. For a symmetrical array and balanced feeding network, an even number of patches across the width of the structure is ideal, with 4 patches allowed on the shorted side. On the longer side, with a length of 400 cm, more latency occurs. Using 50% of the wavelength, the number of patches along the long side is determined to be 21, yielding a total array configuration of 4x21 patches. This results in a total of 84 patches, integrated into the 16 U CubeSat.

C. Feed Network Design

Impedance matching is essential to ensure efficient power transfer between the feed and the antenna, minimizing signal reflections and improving performance. If the impedance of the feed does not match the antenna, power is reflected, increasing the voltage standing wave ratio (VSWR) and reducing the transmitted power, which can degrade the array's gain and signal efficiency. Effective impedance matching optimizes energy transfer, crucial in antenna array design to avoid signal losses and ensure high performance.

Various feeding techniques, such as microstrip line, coaxial probe, and aperture coupling, influence the antenna's impedance matching, bandwidth, and design complexity. For this design, the microstrip feeding method was selected due to its suitability for compact areas, despite its tendency for impedance mismatches. To mitigate this, a quarter-wave transformer (QWT) was applied. The QWT, with a length equal to one-quarter of the signal wavelength, ensures impedance matching or resistive loads between the transmission line and the antenna by using a characteristic impedance that is the geometric mean of the feed and load impedances. This helps cancel any mismatches and ensures optimal energy transfer, and the method is shown in Figure 3.

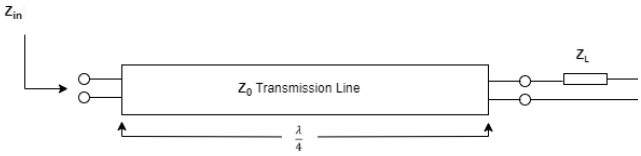

Figure 3 Quarter-Wave Transformer [created by the Author]

D. Series and Parallel Feed Desgin

To achieve a scalable design, where a base array of 4x4 patches can be expanded to a 4xN array, the parallel feed network was selected. Unlike series designs, which need to be tailored to the specific number of patches, parallel configurations offer flexibility. In a series feed network, patches are connected sequentially along a continuous line, with each patch fed in turn, this approach may offer simplicity and lower losses, but for larger arrays, it becomes more complex due to impedance variations as the signal travels through each patch, requiring careful design to ensure uniform power distribution. In contrast, a parallel feed network connects each patch to a central feed line, distributing power equally to all patches, which simplifies the design and makes it more scalable for larger arrays.

III. Results and Discussions

Electromagnetic simulation was used to predict the antenna performance and optimize the design of the patch antenna array. In this paper, CST studio [16] is used to analyze, design, and optimize electromagnetic fields.

A. Design Process - 1x4 Patch Antenna Array

The first design on the 1x1 patch antenna was done using the calculated patch length and width, at a frequency of 1.275 GHz, a dielectric of 3.5, and a total thickness of 2 mm. The PCB was a single layer as shown in Figure 4 below.

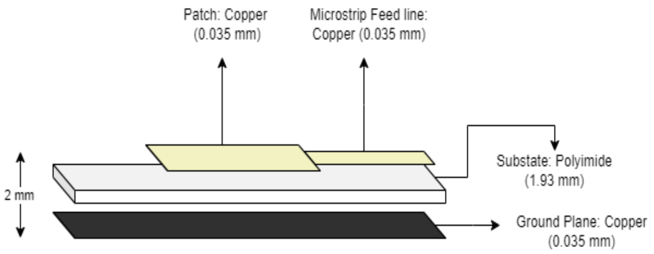

Figure 4 Side view of the PCB [created by the Author]

The first attempt of the CST was not very favorable using the polyimide was challenging, the same design with Rogers as substrate resulted in very low losses and a central frequency of 1.275GHz. However, using polyimide increased the return losses (S_{11}) to a value of -10.81 dB as observed in the next

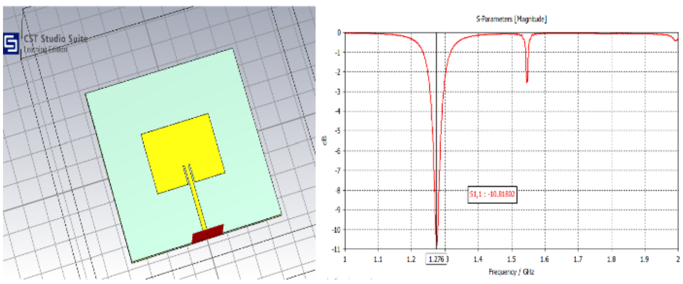

Figure 5 initial trial of CST, 3D schematic of the patch antenna, and the S_{11} resulted.

figure. Using the results obtained, different considerations on the patch design were made to achieve a desirable result.

- Microstrip line length was adjusted to tune the impedance of the patch antenna.
- Patch length and width are responsible for the resonant frequency, input impedance, and radiation efficiency. Required frequency.
- Slots/Notches in patch antenna are often used to improve and modify some of the characteristics of the antenna. In this case, the slot width and length were adjusted, to resonant frequency effectively altering the current path and reducing the effective size of the antenna [4], Figure 6 shows an example of the notches.

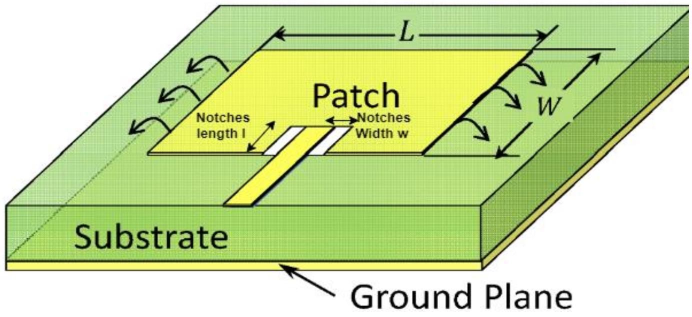

Figure 6 Notches/Slots in Patch antenna [15]

After optimizing the parameters of the antenna, the 1x1 antenna patch resulted in a central frequency of 1.275 GHz, and low return losses of up to -41 dB (ideally).

Table. 1 Optimized Patch antenna array's Parameters and results

Patches #	Patch length (mm)	Patch Width (mm)	QWT (microstrip Line) Impedance (Ω)	QWT (microstrip Line) Width (mm)	QWT (microstrip Line) Length (mm)	Losses (dB)
1	62.40	78.38	N/A			-41
2	62.219	78.2785	N/A			-34.9
3	62.176	78.4036	35.4	7.2305	33.773	-33.4
4	62.176	78.4036	35.4	7.2305	33.773	-34.1
			35.4	7.2305	33.773	

During the optimization process, it was observed that the slight change in patch size resulted in a significant change in the final return losses as shown in Table 1, which implies that the impedance matching was improved. since the quarter wave transformer depends on the length of the microstrip line, it difficult to change, therefore it was kept as a constant throughout the optimization process. The microstrip line between the patch was adjusted to maintain the required element spacing, and in this case, it was 15 cm.

The CST simulation results for return losses were outstanding, especially given that the materials used were anticipated to exacerbate return losses. This demonstrates the design's exceptional ability to mitigate reflections despite the inherent limitations of the materials.

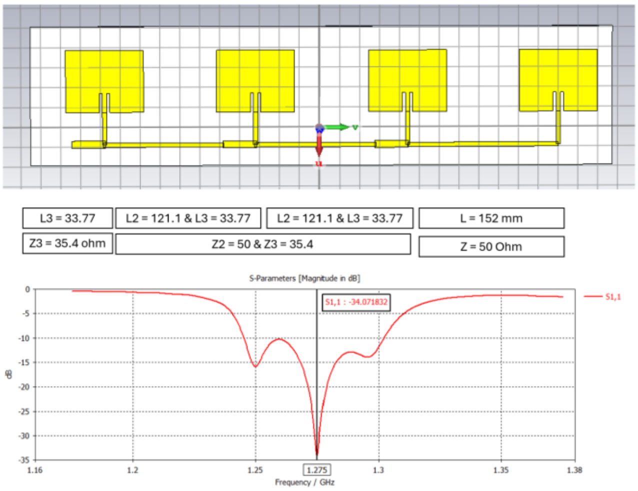

Figure 7 3D schematic of the 1x4 antenna patch, the length and impedance used, and the S_{11} resulted

Figure 7 proves that the design using polyimide as a substrate will not pose a disadvantage to the project. By incorporating the quarter wave transformer between the load impedance of 50 Ω and a 25 Ω input impedance, resulting in a characteristic impedance of 35.35 Ω, achieving a well-matched 1x4 patch antenna array.
Return losses are usually higher for polyimide as they have higher dielectric losses and lower stability compared to the most used rigid PCB materials. This can contribute to an increased signal attenuation and higher return losses for high frequency. However, as demonstrated by the results, this issue can be mitigated through the design of the antenna array, particularly by controlling the impedance [13].

B. *Insitpated Design of 2x4*

The optimization of the 1x4 antenna array has provided a solid foundation for completing the 2x4 antenna array, as both the patch antenna dimensions and the patch spacing have been optimized. As a result, only the microstrip line and the quarter-wave transformer connected to the feeding port require further optimization. Additionally, the previous 1x4 antenna featured

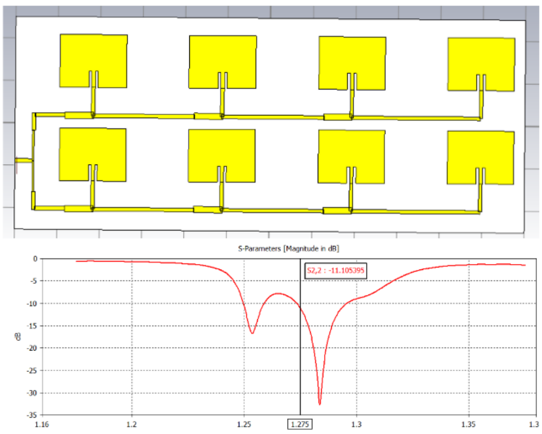

Figure 8 3D schematic of the 2x4 antenna patch, and the S_{11} resulted

a patch spacing of 15 cm, as these antennas were intended to be placed along the longer side of the final array configuration. However, in the 2x4 array case, the spacing has been reduced to meet design constraints, which may lead to reflections and overlaps in the electromagnetic field of the patches.

The results from the 2x4 antenna array will have higher losses, as compared to the 1x4 antenna array by two-thirds, while the results obtained are consistent with the typical results of return losses of a flexible PCB antenna array, which is between -10 dB to -20 dB [14]. However, the design can further be optimized, by either adjusting the microstrip line or increasing the spacing between the patches.

Future Work and Conclusion

The next step in this project involves continuing the optimization of the 2x4 antenna array design to minimize return loss. Following this, we will design the 4x4 antenna array and finalize the PCB layout for prototype production. It is important to note that the bending radius of the array may lead to misalignment in the resulting electromagnetic field. To address this issue, we will introduce a phase shift by adjusting the lengths of the microstrip lines. Since simulations cannot fully capture the effects of the PCB's bending, the printed PCB prototype will be crucial for conducting electromagnetic tests to validate the effectiveness of the design.

The return loss results obtained from CST simulations were remarkably favorable, especially for the 1x4 antenna array, particularly given that the materials used were expected to increase return losses. The observed losses were significantly lower than typical values reported for other flexible materials. This underscores the design's robustness in minimizing signal reflections, despite the anticipated challenges posed by the material properties.

References

[1] Rosen, P.A. *et al.* (2000) 'Synthetic Aperture Radar interferometry', *Proceedings of the IEEE*, 88(3), pp. 333–382. doi:10.1109/5.838084.

[2] Tresoldi, A. *et al.* (2023) 'Development of a deployable synthetic aperture radar antenna for a nanosatellite conceptual design', *Acta Astronautica*, 210, pp. 488–497. doi:10.1016/j.actaastro.2023.04.009.

[3] Tresoldi, A. *et al.* (no date) *Deployer design and testing of a deployable rolled-up composite SAR antenna (DERAC-SAR) for CubeSats*. Available at: https://www.researchgate.net/scientific-contributions/Andrew-C-M-Austin-74927909

[4] Balanis, C.A. (2016) *Antenna theory: Analysis and design, 4th Edition*, *Wiley.com*. Available at: https://www.wiley.com/en-es/Antenna+Theory%3A+Analysis+and+Design%2C+4th+Edition-p-9781118642061

[5] "National Frequency Plan," Telecommunications and Digital Government Regulatory Authority (TDRA), available: https://tdra.gov.ae/en/test/national-frequency-plan.

[6] *Seasat* (no date) *NASA*. Available at: https://www.jpl.nasa.gov/missions/seasat

[7] "16U Structure," EnduroSat, available: https://www.endurosat.com/products/16u-structure/.

[8] A. Doerry, "Introduction to Synthetic Aperture Radar," 2019 IEEE Radar Conference (RadarConf), Boston, MA, USA, 2019, pp. 1-90, doi: 10.1109/RADAR.2019.8835560.

[9] M. I. Skolnik, "Radar Handbook", 3rd ed., New York, NY, USA: McGraw-Hill, 2008.

[10] MDA announces RADARSAT-2 Continuity mission (no date) MDA Announces RADARSAT-2 Continuity Mission | MDA Space. Available at: https://mda.space/article/mda-announces-radarsat-2-continuity-mission

[11] S1 applications (no date a) Explore Copernicus satellite missions - Sentinel Online. Available at: https://sentinel.esa.int/web/sentinel/user-guides/sentinel-1-sar

[12] *Bend Radius: FPC bendability -flex PCB manufacturer* (2021) *MADPCB*. Available at: https://madpcb.com/glossary/bend-radius/.

[13] J. Fjelstad, ‘Flexible Circuit Technology’, 4th ed., Minneapolis, MN, USA: BR Publishing, 2011.

[14] Khade, V. and Wuppulluri, M. (2023) ‘A comparative study on rigid and Flexible Magnetoelectric Composites: Review’, *Journal of Advanced Dielectrics*, 14(02). doi:10.1142/s2010135x23400015.

[15] Ke, L., Liu, Z. and Yu, H. (2018) ‘Characterization of a patch antenna sensor’s resonant frequency response in identifying the notch-shaped cracks on metal structure’, *Sensors*, 19(1), p. 110. doi:10.3390/s19010110.

[16] CST Studio Suite, version 2019, Dassault Systèmes, 2019. [Online]. Available: https://www.3ds.com/products-services/simulia/products/cst-studio-suite/